CHAPTER – II

PREPARATION AND CHARACTERIZATION OF FERRITE SAMPLES

PART – A

PREPARATION OF FERRITE SAMPLES

2.1 INTRODUCTION

The properties of ferrites are sensitive to the structural aspects like grain size, porosity and orientation of the grains. They also depend upon the purity of the starting compounds and in general on the physico-chemical history of the ferrites. So the properties of the ferrites can be controlled by the process techniques. Efforts are being made to prepare ferrites by various methods [1,2,3]. Hilpert [4], in 1909, recognised the importance of oxide magnetic meterials and investigated the solid state reaction leading to the ferrite formation. The modern theory of preparation of spinel ferrites was first introduced by Wagner [5] and further developed by Schmalzried [6] and Hauffe [7]. Philips, Netherland developed the process for the formation of commercial ferrites. The details are given by Snoek [8].

There are two important methods of preparation of ferrites. The chemical methods are advantageous as far as the control of grain size is concerned. Due to some limitations of the chemical methods most of the time standard

ceramic technique is preferred. The ceramic method enables to prepare ferrites with desired chemical composition, shape and microstructure. This method is relatively simpler and cheap. And again, whether we start from mixture prepared by chemical method or by ceramic method, we must resort to heat treatment for sintering. We have prepared the ferrites by ceramic method [9,10,11] by allowing the component oxides to react at elevated temperature.

2.2 MECHANISM OF SOLID STATE REACTION

In ceramic method the solid state reaction plays important role in the formation of spinel ferrites and it can be discussed on the basis of diffusion of components involving divalent metal oxide Mo and Fe_2O_3. In the initial configuration there is only one phase boundry between the reactants. After the nucleation of the ferrites, the boundry is replaced by different phase boundaries, one between Mo and ferrite MFe_2O_4 and another between Fe_2O_3 and MFe_2O_4. In this stage further progress of the reaction can only take place by transport of reactants through the ferrite phase. There are three possible mechanisms. In the counter diffusion mechanism suggested by Wagner [12], only cations migrate in the opposite directions, the oxygen ions are essentially stationary. In the second mechanism the anions take part in the diffusion process. In this reaction, diffusion of one cation is compensated by an associated flux

of anions (O^{2+}) instead of a counter current of another cation. In the third mechanism iron is diffused through the ferrite layer in the reduced state Fe^{2+}. In such a case oxygen is transported through the gas phase, being given off at MFe_2O_4/Fe_2O_3 interface and taken up again at Mo/MFe_2O_4 boundary.

2.3 PREPARATION OF FERRITES

In the preparation of ferrites by ceramic method, the starting materials are allowed to undergo solid state reaction reaction. Basically, four steps are involved in this process.

(i) Preparation of material to form an intimate mixture with the metal ions in the required ratio for final product.

(ii) Presintering or calcination.

(iii) Powdering of presintered material, and pressing to form the required shape.

(iv) sintering to form the final product.

The general ceramic method of ferrite preparation can be represented by a 'flow chart' shown in figure 2.1.

2.3.1. *METHODS OF PREPARATION OF FERRITE COMPOSITION*

There are four general methods for preparation of ferrite ferrite compositions. They are as follows.

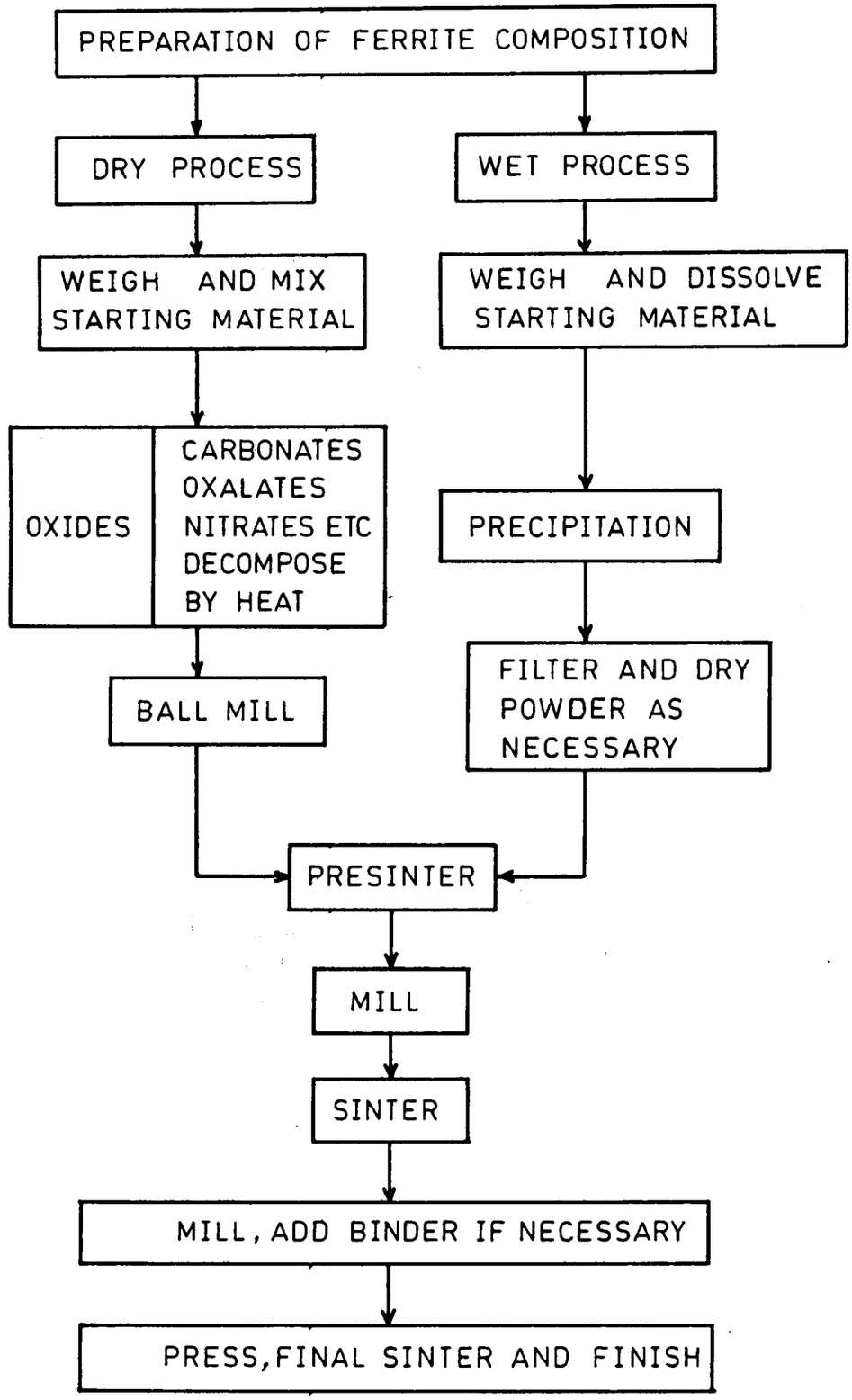

FIG·2·1 FLOW CHART OF STAGES IN THE FERRITE PREPARATION.

(a) *OXIDE METHOD*

This is the most extensively used method in the commercial production of ferrites, which requires little chemical knowledge. High purity oxides of metals in the required proportion for final product are mixed together. After milling, the mixture is dried and fixed at a moderately low temperature (500 – 700°C), and the resulting material is again broken up and milled before final sintering is done. This is repeated several times to obtain a high degree of homogeneity.

(b) *DECOMPOSITION METHOD*

In this method, instead of using oxides as starting materials, salts like carbonates, nitrates and oxalates are used. These salts are mixed by milling in the appropriate proportions and then preheated in air so as to form oxides by thermal decomposition. The oxides formed by this method have ability to undergo solid state reactions readily [13]. The other details of the method are similar to the oxide method.

(c) *HYDROXIDE PRECIPITATION*

This method is useful in order to avoid the lengthy milling process involved in dry mixing. The method is based upon simultaneous precipitation of required oxides from solution. The essential requirements of the method are :

knowledge of solubility product and quantitative understanding of the chemical process.

(d) *OXALATE METHOD*

This method is preferred for two reasons. Firstly, precipitation can be carried out using ammonium oxalate which does not have any residue, and secondly, most of the metal oxalates are very similar in crystal structure. Therefore, precipitation tends to produce mixed crystals which contain the metallic cations in the proportion in which they were present in the solution. Thus mixing in the correct ratios can be achieved on a molecular scale [14].

2.3.2. *PRE SINTERING*

Pre sintering is a slow solid state reaction in which reactants partly react to form final product. The amount of reaction depends upon reactivity of components as well as the pre sintering temperature [15]. The purpose of pre sintering is to decompose carbonates and higher oxides in order to reduce the evolution of gas in the final sintering process. It assists in homogenizing of the material and also to reduce the variations in the composition of raw materials. Pre sintering is necessary to control the shrinkage of the material which occurs during final sintering.

2.3.3. *POWDERING AND PRESSING*

The pre sintered meterial is powdered by milling. The compact and desired shape of the material is done by high pressure technique, employing a pressure of several tons per sq. inch. The compacted material is finally subjected to sintering.

2.3.4. *SINTERING*

Sintering consists of heating of the compacted material at high temperature. Sintering in crystalline solids has been dealt with in detail by Coble and Burke [18]. Sintering occurs in three stages :

(1) Initial stage – Here atomic diffusion can quantitatively account for the initial rate of neck growth between pairs of spheres. Grain growth is totally inhibited.

(2) Intermediate stage – When the density is approximately 60% of its theoretical value, grain growth sets in. The structure still has a completely continuous pore phase. The density increases with the logarithm of time. The densification rate decrease somewhat due to an increase in grain size. Lattice vacancies can be discharged only at the grain boundaries. At about 95% of the theoretical density the pore phase becomes discontinuous, terminating the intermadiate stage.

(3) Final stage - If discontinuous grain growth occurs, a large number of pores trapped inside the grains and isolated from the grain boundaries, cannot shrink any more. Then sintering is practically stopped. If discontinuous grain growth can be avoided, the last few percent of porosity are eliminated by discharging vacancies at grain boundaries. The compact then sinters to a high density.

2.4. HOT PRESSING

Hot pressing technique involves the enhancement of densification by simultaneous application of high pressure and temperature [16]. The application of pressure serves to augment the normal driving force for densification and thus makes possible the use of lower sintering temperatures. The main factors affecting the hot pressing process are temperature, time, pressure, particle characteristic and environment.

The application of pressure assists densification process so that the required densification is obtained in a short time. The most important advantage of this technique is that it provides the possibility of suppressing grain growth which takes place more rapidly at higher temperature. This technique has significant control over the microstructure [17]. The selection of 'hot pressing' is desirable for very stringent microstructure control in

addition to the requirement of high density.

An improved version of hot pressing known as 'continuous hot pressing' [19] enables to conserve the original particle size of the starting powder and to combine this with a very low porosity.

2.5. ACTUAL PREPARATION OF FERRITE SAMPLES

Mixed Cobalt Zinc ferrites were prepared by standard ceramic technique. The details of the steps involved are as follows :

(a) *GENERAL FORMULA*

The general formula for the ferrite system is

$$Co_xZn_{1-x}Fe_2O_4$$

where $x = 0, 0.2, 0.4. 0.6, 0.8$ and 1.0.

(b) *STARTING MATERIALS*

The AR grade cobalt oxide (CoO). Zinc oxide (ZnO) and ferric oxide (Fe_2O_3) were used as starting materials.

(c) *WEIGHING*

In order to prepare each sample of 10 gms, the requisite oxides were weighed on a semimicrobalance according to molecular percentage.

(d) *PRE SINTERING*

The compositional weights of powders were mixed physically and blended in an agate morter in acetone medium.

The mixture was allowed to dry in air. The mixture of each sample was pre sintered in a platinum crucible at 800°C for 20 hrs.

The pre sintered powders were subjected to hand milling process in acetone medium for 6 hrs. The dried powders were sieved to eliminate bigger particles.

(e) *PELLET FORMATION*

To prepare a pellet, a small quantity (≈ 1 gm) of powder was ground in acetone by adding few drops of polyVinyl Acetone (PVA). The mixture was allowed to dry in air. With the help of a die of 1 cm. in diameter, pellets were formed by subjecting dried powder to a hydraulic pressure of about 10 tons for 5 minutes.

(f) *FINAL SINTERING*

The pellets were subjected to final sintering by keeping them on platinum sheets. The final sintering was carried out in a silicon carbide furnace, at 900°C temperature. Chromel-Alumel thermocouple was used to measure the temperature of the furnace. As it is desired to study the effect of sintering time pellets of each sample were sintered at 900°C for 15 hrs and 30 hrs respectively. Pellets were furnace cooled at the rate of about 80°C/hr.

PART – B

CHARACTERIZATION OF FERRITE SAMPLES BY X-RAY DIFFRACTION TECHNIQUE.

2.6 INTRODUCTION

The X-ray diffraction technique is an esteemed and well established tool for the study of the crystal structures. Since X-rays can penetrate solids non-destructively the diffraction of X-rays provides information about the internal structure of crystals. Here this technique is used to confirm the spinel structure of ferrites and the completion of solid state reaction during their preparation, and also to determine the lattice parameter of spinel structure.

2.7. X-RAY DIFFRACTION

The simplest explanation of the observed diffraction pattern that results from the passage of X-rays through the crystal was first given by Bragg [20]. It was shown by Bragg that diffraction maxima occur when the Bragg's law

$$2d \sin \theta = n\lambda \qquad \ldots (2.1)$$

where n = order of diffraction,

λ = wave length of X-rays

and d = interplanar distance

is satisfied.

If (hkl) are the Miller indices for a set of parallel planes, for cubic system the interplanar distance is given by

$$d = \frac{a}{\sqrt{h^2 + k^2 + l^2}} \; n \qquad \ldots (2.2)$$

From equations (2.1) and (2.2) we get, for lattice parameter

$$a = \frac{\lambda \sqrt{h^2 + k^2 + l^2}}{2 \text{ Sin } \theta} \qquad \ldots (2.3)$$

Monochromatic X-rays of wavelength λ striking a 3-dimensional crystal at an arbitrary angle of incidence will not in general be reflected. To satisfy Bragg's condition and to cause diffraction we have to vary either wave length (λ) or angle of incidence (θ). There are three methods of crystal analysis by X-rays.

(a) *LAUE METHOD*

Here a single crystal is kept stationary in a beam of X-rays of continuous wave lengths. The crystal selects and diffracts descrete values of λ satisfying Bragg's condition.

(b) *ROTATING CRYSTAL METHOD*

Here a single crystal is rotated in a beam of monochromatic X-rays. Variation in θ brings different atomic planes into position for reflection.

(c) *POWDER METHOD*

The powder method of X-ray diffraction was first developed by Debye and Scherrer [21] in 1916. In this method the incident monochromatic radiation of wavelength (λ) strikes a finely powdered specimen or a fine grained polycrystalline specimen contained in a thin walled capillary tube. The distribution of crystallites orientations will be nearly continuous. The powder method is convenient precisely because single crystals are not required. Diffracted rays go out from individual crystallites that happen to be oriented with planes making an incident angle θ with the beam satisfying the Bragg's equation. Diffracted rays leave the specimen along the generators of cones concentric with the direction of the original beam. The generators make angle of 2θ with the direction of the original beam, where θ is the Bragg angle. The cones intercept the film in a series of concentric rings (figure 2.2). By measuring the radius of the ring and the radius of the cylindrical film, the angle 2θ and hence θ can be determined. Using Bragg's Equation 2.1, interplanar distance d can be computed.

In X-ray diffractometer, a counter is mounted instead of a film. The counter gives graphical record which is proportional to the intensity of diffracted radiation.

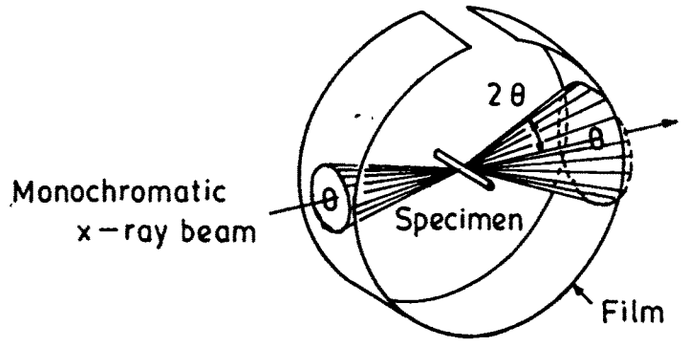

FIG. 2·2 - BRAGG'S PRINCIPLE OF X-RAY POWDER DIFFRACTION.

2.8 EXPERIMENTAL

The X-ray diffraction pattern of ferrite system $Co_xZn_{1-x}Fe_2O_4$ with x = 0, 0.2, 0.4, 0.6, 0.8, and 1.0 were obtained from Indian Institute of Science, Bangalore. All samples were in the form of fine powders, and Fe K_α-radiation of wave length 1.93604 A^o was used. The diffractograms were taken with in the range of 2θ angle between 10° and 85°. The patterns were analysed by usual method. For $ZnFe_2O_4$ alone λ was 1.542 A^o.

2.9 INDEXING DIFFRACTION MAXIMA AND CALCULATION OF LATTICE PARAMETERS

In an XRD pattern of any spinel ferrite the peak [311] is very prominent, and can be identified easily. The corresponding values of 2θ is noted from the diffractogram. Using the values of θ, (hkl) and λ , from equation 2.3 lattice parameter 'a' can be calculated. Once the value of 'a' is known, the indices of other planes can be readily decided by the usual method. If we consider any other peak with $2\theta = x$ (say), Equation 2.3 gives $(h^2 + k^2 + l^2)$ and hence (hkl) value. Similarly indices for all other peaks may be decided.

From Equations 2.2 & 2.1 the interplanar distance d_c (theoretical) and d_o (experimental) are calculated and compared.

2.10 RESULTS AND DISCUSSION

The X-ray diffractograms of the $Co_xZn_{1-x}Fe_2O_4$ system are given in Figs. 2.3 - 2.8. The well defined X-ray dffractogram peaks show a perfect crystalline nature of our samples.

Ferrites are spinels and have the following reflections for cubic structure [22];

(111),(220),(311),(222),(400),(422),(511), and (440).

With our samples we have observed above mentioned reflections for cubic structure. This confirms the structure and formation of ferrites.

For a cubic structure, the cyclic sum of the indices i.e. (h+k), (k+1), and (l+h) should come out to be an even integer. This is strictly observed for all the planes and for all the compositions. It indicates cubic nature of the ferrite system under study.

The d-values, corresponding planes of reflections (hkl), crystal structure and lattice parameter are given in Tables 2.1 - 2.6. Fig. 2.9 shows variation of lattice parameter with the compositional variation of Zn in the ferrite system. It can be seen that the lattice parameter increases linearly with Zn-content in the system. Lattice parameter has a min. value (= 8.39 A^o) for $CoFe_2O_4$, and a max. value (= 8.44 A^o) for $ZnFe_2O_4$ max. These values of 'a' are in good agreement

with previously reported values [24]. A linear relation is established, and this shows that Vegard's law [23] is obeyed by our samples. Since the ionic radius of Zn (0.83 A^o) is greater than that of Co (0.78 A^o) [25], the ionic volume of Zn is greater than that of Co. Therefore it is expected that the lattice parameter should increase linearly with Zn content in the ferrite sample.

The data on X-ray and physical densities of different $CoZn_{1-x}Fe_2O_4$ compositions are given in table 2.7. It can be seen that the physical densities differ from and are smaller than the X-ray density. This is attributed to the porosity prevailent in final processed pellets. Actual density shows small decrease with increasing Zn content in the composition. This is obvious as Zn is lighter (SG =7.14) than Co(SG = 8.9).

Table 2.8 gives bond lengths R_A and R_B, and site radii r_A and r_B for different ferrite compositions. Figs. 2.10 and 2.11 show variation of average bond length R_A and R_B against the Zn content in the system $Co_xZn_{1-x}Fe_2O_4$. The values of R_A and R_B are calculated by using the relations

$$R_A = \sqrt{3} \quad a \left[\frac{1}{8} + \delta \right]$$

and

$$R_B = a \sqrt{\frac{1}{16} - \frac{\delta}{2} + 3\delta^2}$$

BARR. BALASAHEB KHARDEKAR LIBRARY
SHIVAJI UNIVERSITY, KOLHAPUR.

where R_A and R_B are the shortest distances between A-site cation and oxygen ions, and B-site cation and oxygen ions respectively, and $\delta = u - 0.375$, the deviation from oxygen parameter. u-values for mixed ferrite samples are calculated from those for simple ferrites already reported in crystallographic data for spinels [26]. From Fig. 2.10 it is seen that R_A increases linearly with the increase of Zn content in $Co_xZn_{1-x}Fe_2O_4$ system. The value of R_A is minimum for $CoFe_2O_4$ and maximum for $ZnFe_2O_4$.

The increase in bond length R_A can be associated with the increase in the lattice parameter 'a' in the system with the increase in the content of Zn. Since $ZnFe_2O_4$ is a normal spinel and Zn^{2+} ions have preference for A-site, the amount of Zn^{2+} ions on A-site increases with the increase in Zn content in the $Co_xZn_{1-x}Fe_2O_4$ system. The increase of bond length R_A with more content of Zn^{2+} in the system is in accordance with this relation.

From Fig. 2.11 it is seen that as the Zn content in the ferrite system $Co_xZn_{1-x}Fe_2O_4$ increases the bond length R_B decrases. The value of R_B is maximum for $CoFe_2O_4$ and minimum for $ZnFe_2O_4$. Levine [27] has shown that there exists an inverse relationship between the covalent character of

spinel and the bond length. The compositional variation of R_B suggests that the ionocovalent character of bonding increases with the content of Zn. As Zn^{2+} occupies A-site only and bonding between Fe^{3+} ions on B-site being ionic, it is the partial ionic bonding between Co^{2+} ions on B-sites that lends ionocovalent character to the mixed system. The nature of variation of the bonding can be discussed on the basis of crystal field splitting as suggested by Dunitz and Orgel [28].

We have also calculated the radius of A and B sites in case of our samples using the formulae given by Smit and Wijn, viz

$$r_A = \sqrt{3}\ a\ (u - \tfrac{1}{4}) - r(O^{2-}),$$

$$r_B = a\ (\tfrac{5}{8} - u) - r(O^{2-}),$$

Where u = oxygen parameter of ferrite

and $r(O^{2-})$ = Goldsmit radius of O^{2-}

= 1.35 A^o

Fig. 2.12 and 2.13 represent the compositional variation of r_A and r_B with content of Zn in the system $Co_xZn_{1-x}Fe_2O_4$. For our samples radius of A-site varies from 0.54 A^o (for $CoFe_2O_4$) to 0.62 A^o (for $ZnFe_2O_4$); and radius

of B-site varies from 0.67 A^{o} (for $ZnFe_2O_4$) to 0.69 A^{o} (for $CoFe_2O_4$). The Goldsmith ionic radii for Co^{2+}, Zn^{2+}, Fe^{3+} and Fe^{2+} ions are 0.78 A^{o}, 0.83 A^{o}, 0.67 A^{o} and 0.80 A^{o} respectively. Hence it can be concluded that the site radii r_A of A-sites appear to be too small to admit the ions without local distortion of site or ion, or both.

TABLE - 2.1

X-Ray Diffraction data of $CoFe_2O_4$ ferrite.
Wave length, λ = 1.93604 A° ,
Average lattice Parameter , a = 8.3915 A° ,
Structure - cubic.

S.No.	2 θ in degree	(hkl)	dc in A° (calculated)	do in A° (observed)
1	23	(111)	4.8437	4.8554
2	38.1	(220)	2.9661	2.9658
3	45	(311)	2.5295	2.5295
4	47.1	(222)	2.4218	2.4227
5	55.1	(400)	2.0974	2.0929
6	68.8	(422)	1.7125	1.7134
7	73.6	(333)	1.6145	1.6159
8	81.5	(440)	1.4830	1.4829

TABLE - 2.2

X-Ray Diffraction data of $Co_{0.8}Zn_{0.2}Fe_2O_4$ ferrite.
Wave length, λ = 1.93604 A° ,
Average lattice Parameter , a = 8.3995 A° ,
Structure - cubic.

S.No.	2 θ in degree	(hkl)	dc in A° (calculated)	do in A° (observed)
1	38.0	(220)	2.9693	2.9658
2	44.95	(311)	2.5322	2.5322
3	47.1	(222)	2.4244	2.4228
4	55.0	(400)	2.0996	2.0964
5	68.7	(422)	1.7153	1.7156
6	73.5	(333)	1.6163	1.6179
7	81.4	(440)	1.4846	1.4845

TABLE - 2.3

X-Ray Diffraction data of $Co_{0.6}Zn_{0.4}Fe_2O_4$ ferrite.
Wave length, λ = 1.93604 A° ,
Average lattice Parameter , a = 8.4084 A° ,
Structure - cubic.

S.No.	2 θ in degree	(hkl)	dc in A° (calculated)	do in A° (observed)
1	38.0	(220)	2.9724	2.9733
2	44.9	(311)	2.5349	2.5349
3	47.0	(222)	2.4269	2.4276
4	54.9	(400)	2.1018	2.0999
5	68.6	(422)	1.7161	1.7177
6	73.5	(333)	1.6179	1.6179
7	81.25	(440)	1.4862	1.4867

TABLE - 2.4

X-Ray Diffraction data of $Co_{0.4}Zn_{0.6}Fe_2O_4$ ferrite.
Wave length, λ = 1.93604 A° ,
Average lattice Parameter , a = 8.4203 A° ,
Structure - cubic.

S.No.	2 θ in degree	(hkl)	dc in A° (calculated)	do in A° (observed)
1	37.95	(220)	2.9787	2.9771
2	44.8	(311)	2.5403	2.5403
3	47.0	(222)	2.4321	2.4276
4	54.75	(400)	2.1063	2.1052
5	68.6	(422)	1.7197	1.7199
6	73.4	(333)	1.6214	1.6198
7	81.1	(440)	1.4894	1.4890

TABLE - 2.5

X-Ray Diffraction data of $Co_{0.2}Zn_{0.8}Fe_2O_4$ ferrite.
Wave length, λ = 1.93604 A°,
Average lattice Parameter, a = 8.4313 A°,
Structure - cubic.

S.No.	2θ in degree	(hkl)	dc in A° (calculated)	do in A° (observed)
1	37.90	(220)	2.9813	2.9808
2	44.75	(311)	2.5424	2.5424
3	46.9	(222)	2.4342	2.4325
4	54.70	(400)	2.1080	2.1071
5	68.4	(422)	1.7212	1.7222
6	73.25	(333)	1.6228	1.6341
7	80.9	(440)	1.4906	1.4920

TABLE - 2.6

X-Ray Diffraction data of $ZnFe_2O_4$ ferrite.
Wave length, λ = 1.542 A°,
Average lattice Parameter, a = 8.4424 A°,
Structure - cubic.

S.No.	2θ in degree	(hkl)	do in A° (calculated)	do in A° (observed)
1	18.2	(111)	4.8691	4.8748
2	29.9	(220)	2.9817	2.9886
3	35.3	(311)	2.5428	2.5428
4	36.9	(222)	2.4345	2.4361
5	42.8	(400)	2.1084	2.1134
6	53.15	(422)	1.7215	1.7234
7	56.65	(333)	1.6230	1.6249
8	62.3	(440)	1.4908	1.4904

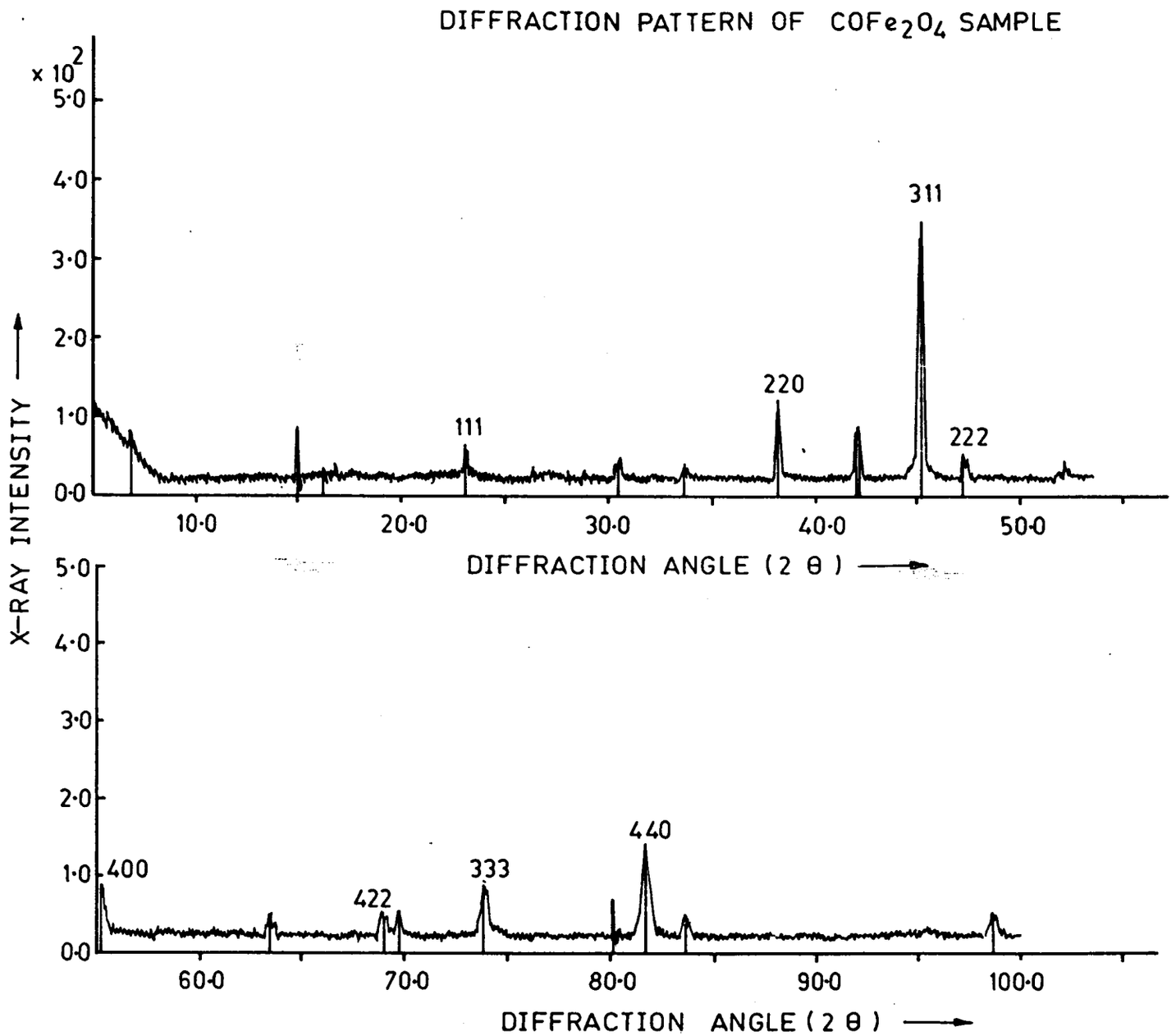
DIFFRACTION PATTERN OF $COFe_2O_4$ SAMPLE
x 10^2
5·0
4·0
3·0
2·0
1·0
0·0
X-RAY INTENSITY
111
220
311
222
10·0
20·0
30·0
40·0
50·0
DIFFRACTION ANGLE (2 θ)
400
422
333
440
60·0
70·0
80·0
90·0
100·0
DIFFRACTION ANGLE (2 θ)

Fig. 2·3

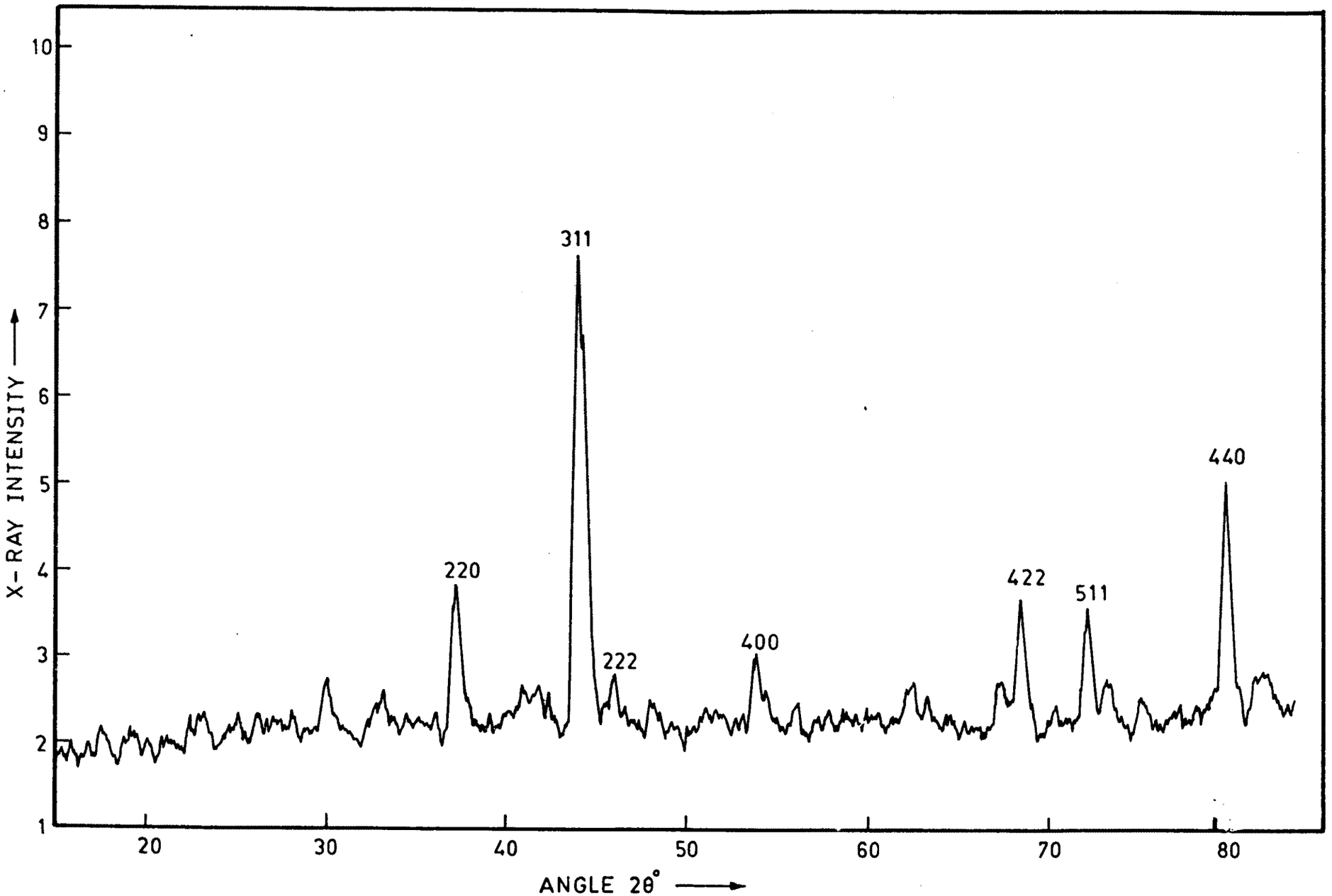

FIG.2·4 - X-RAY DIFFRACTION PATTERN OF $Co_{0\cdot8}Zn_{0\cdot2}Fe_2O_4$.

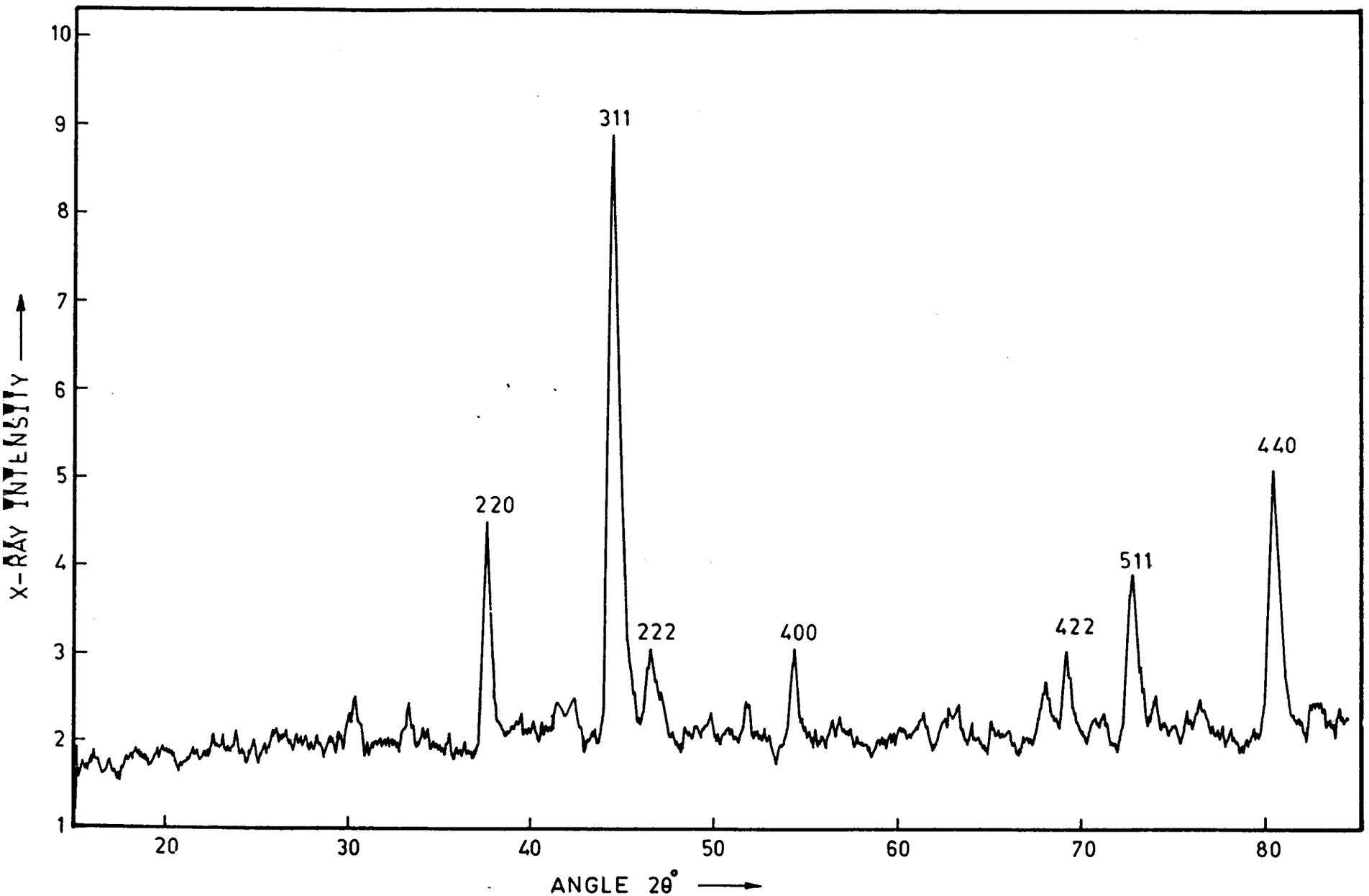

FIG. 2·5 - X-RAY DIFFRACTION PATTERN OF $Co_{0.6}Zn_{0.4}Fe_2O_4$.

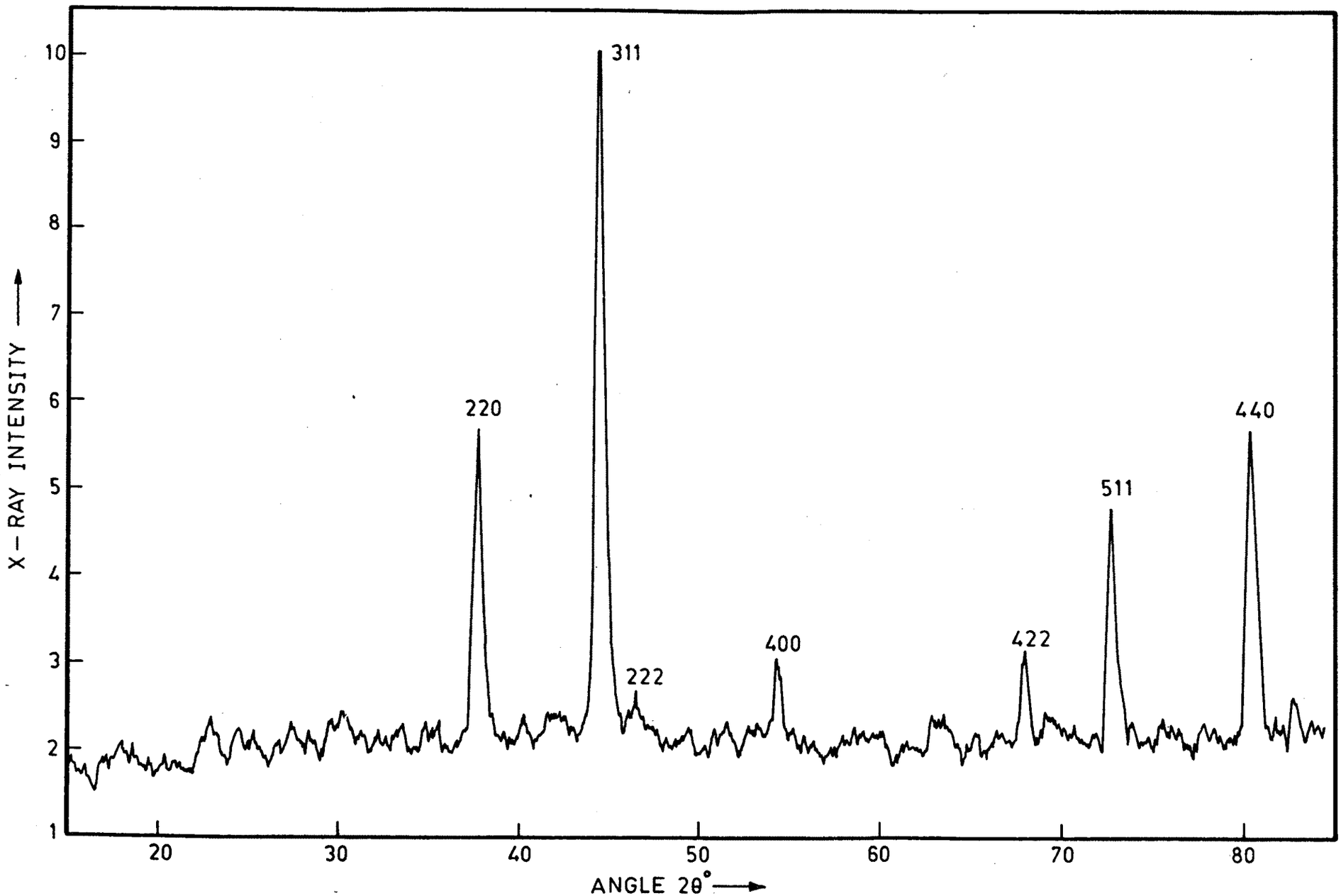

FIG.2·6- X-RAY DIFFRACTION PATTERN OF $Co_{0\cdot4}Zn_{0\cdot6}Fe_2O_4$.

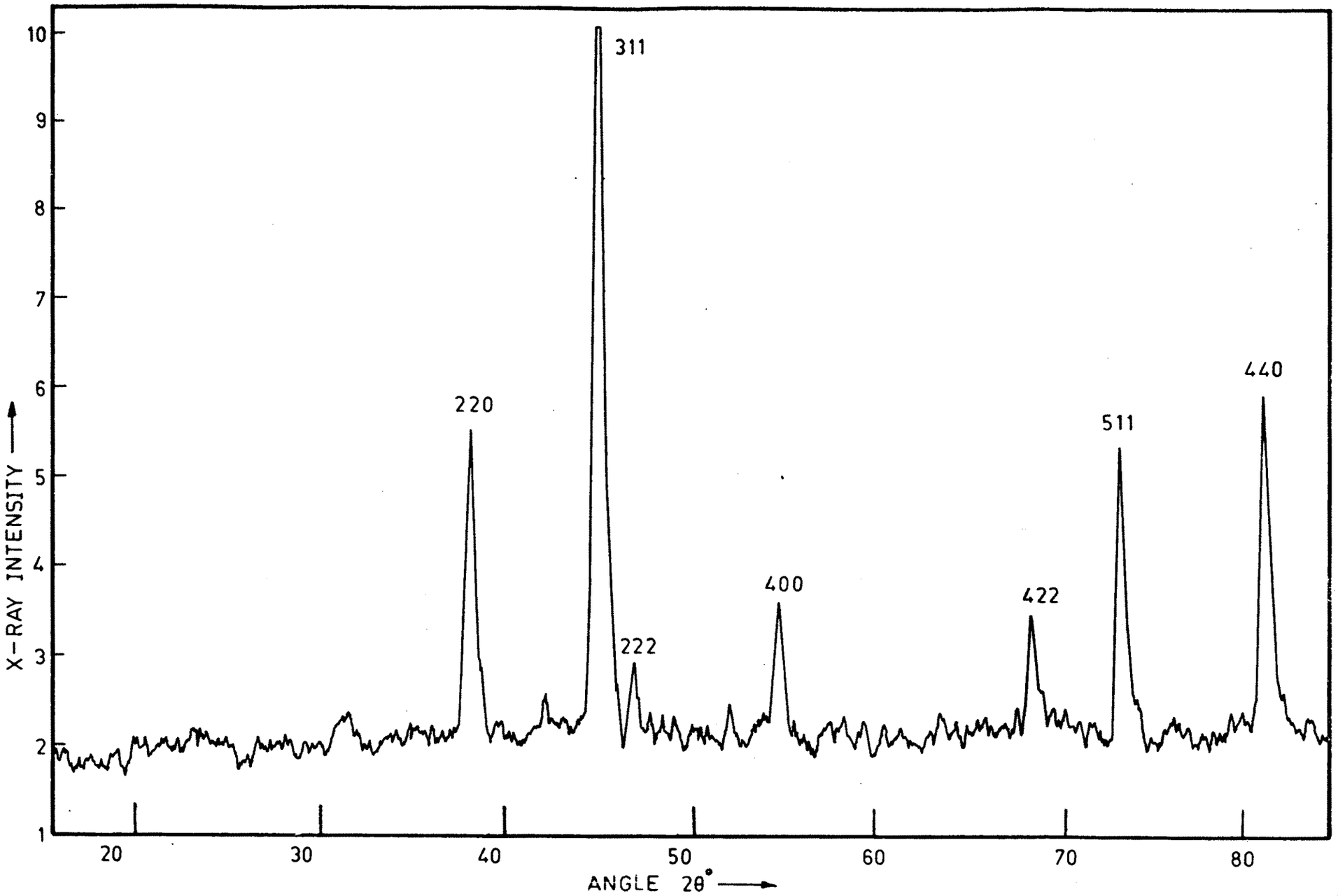

FIG. 2·7- X-RAY DIFFRACTION PATTERN OF $Co_{0.2}Zn_{0.8}Fe_2O_4$

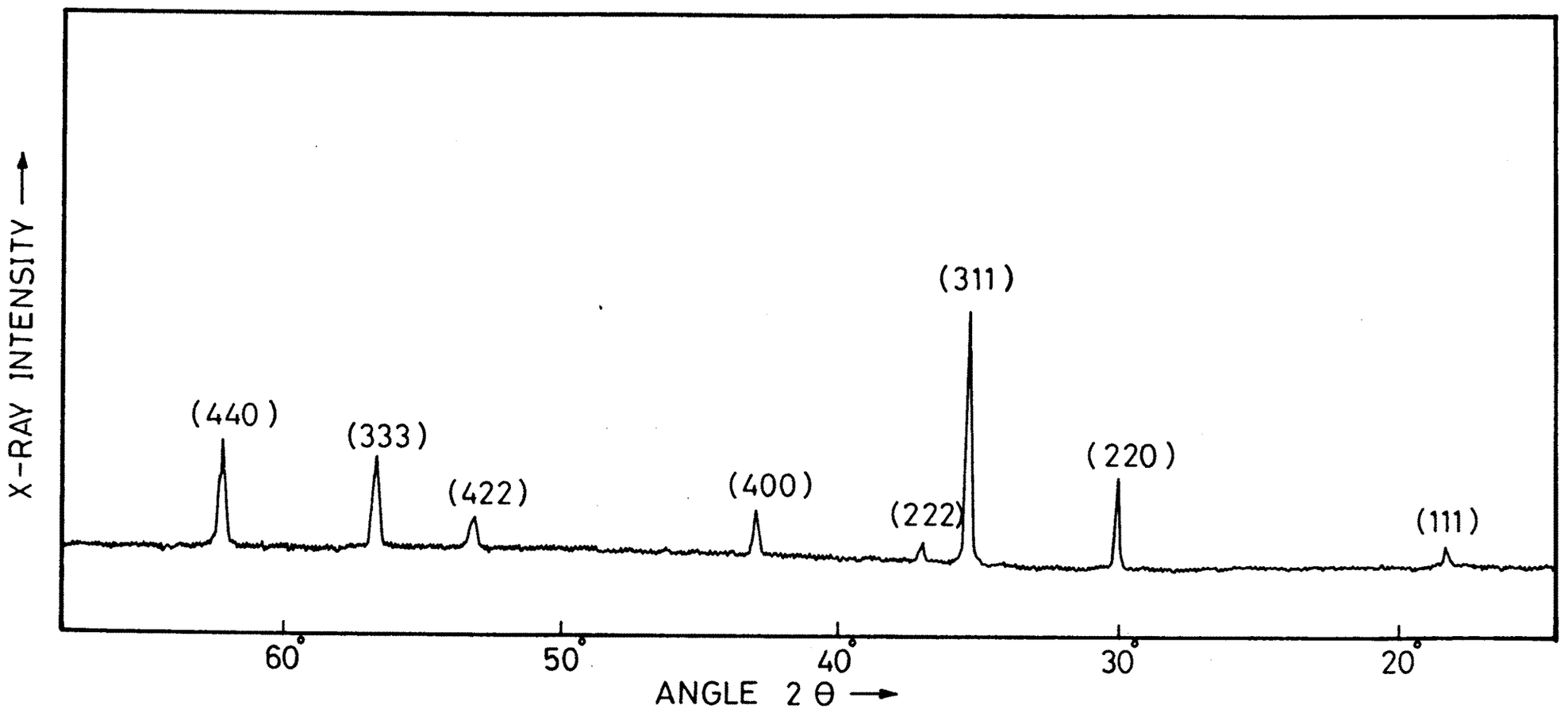

Fig.2·8- X-Ray diffraction pattern of $ZnFe_2O_4$

TABLE - 2.7

Physical density, X-ray density and Porosities of $Co_xZn_{1-x}Fe_2O_4$ samples Sintered at 900°c for 15 hrs and 30 hrs.

S.No.	Composition	Sintering time hrs.	Molecular weight M	Lattice Parameter a,A°	Physical density d_m,gms/cc	X-ray density dx	Porosity P
1	$CoFe_2O_4$	15	233.67	8.3915	4.02	5.253	0.234
		30			4.14		0.216
2	$Co_{0.8}Zn_{0.2}Fe_2O_4$	15	234.958	8.3995	3.91	5.267	0.257
		30			4.04		0.233
3	$Co_{0.6}Zn_{0.4}Fe_2O_4$	15	236.245	8.4084	3.83	5.279	0.274
		30			3.91		0.259
4	$Co_{0.4}Zn_{0.6}Fe_2O_4$	15	237.533	8.4203	3.70	5.285	0.299
		30			3.81		0.279
5	$Co_{0.2}Zn_{0.8}Fe_2O_4$	15	238.820	8.4313	3.59	5.293	0.321
		30			3.73		0.294
6	$ZnFe_2O_4$	15	240.107	8.4424	3.50	5.301	0.339
		30			3.61		0.318

TABLE - 2.8

Average bond lenth R_A & R_B and site radii r_A & r_B of different CoZn ferrite samples.

S.No.	Composition	Lattice Parameter 'a' in A°	U-Value in A°	R_A in A°	R_B in A°	r_A in A°	r_B in A°
1	$CoFe_2O_4$	8.3915	0.3810	1.9016	2.0488	0.5540	0.6975
2	$Co_{0.8}Zn_{0.2}Fe_2O_4$	8.3995	0.3818	1.9175	2.0444	0.5575	0.6928
3	$Co_{0.6}Zn_{0.4}Fe_2O_4$	8.4084	0.3826	1.9312	2.0402	0.5812	0.6882
4	$Co_{0.4}Zn_{0.6}Fe_2O_4$	8.4203	0.3834	1.9456	2.0368	0.5956	0.6843
5	$Co_{0.2}Zn_{0.8}Fe_2O_4$	8.4313	0.3842	1.9598	2.0332	0.6098	0.6803
6	$ZnFe_2O_4$	8.4424	0.3850	1.9741	2.0297	0.6241	0.6762

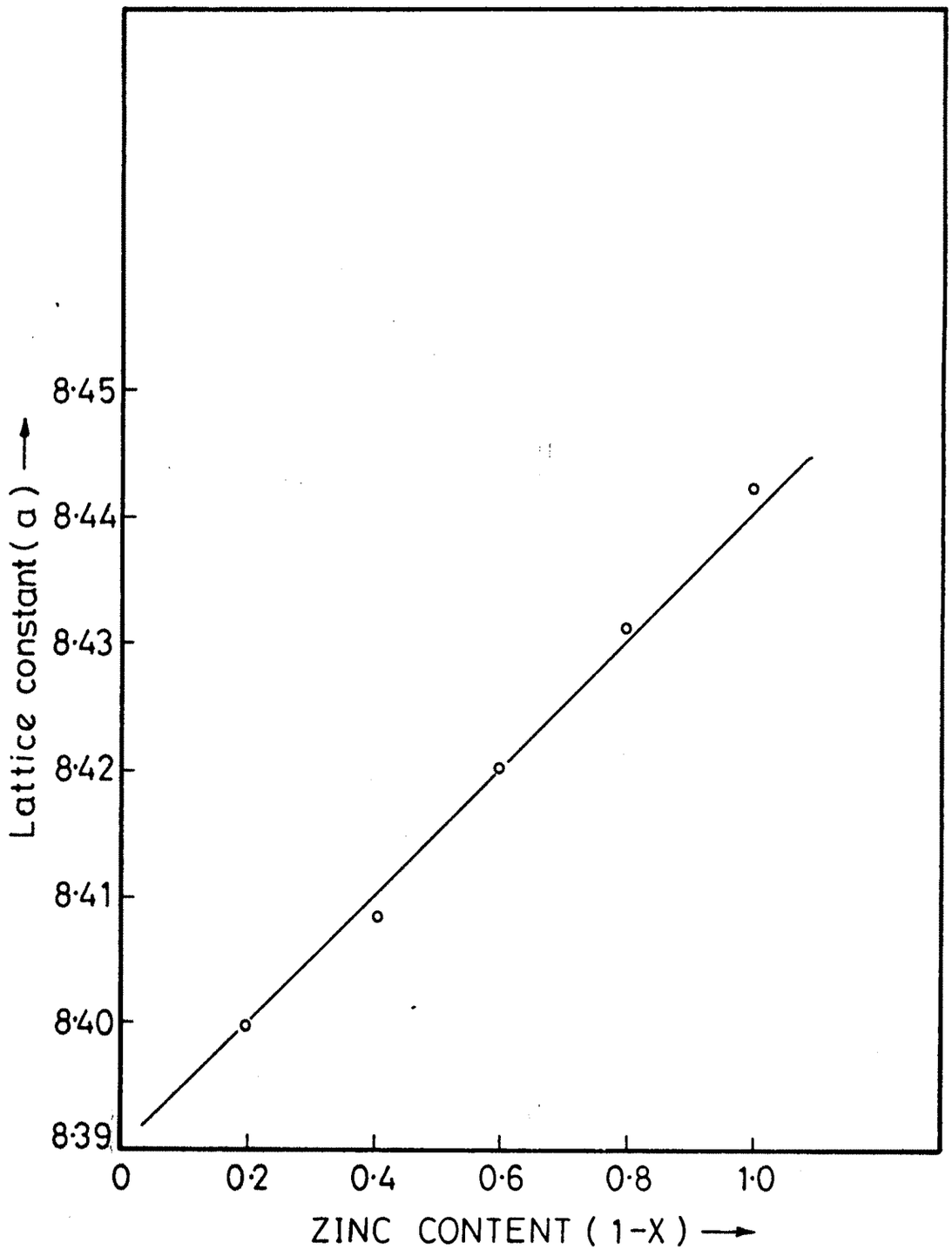

Fig. 2·9-Variation of the lattice constant of $Co_xZn_{1-x}Fe_2O_4$ with zinc concentration.

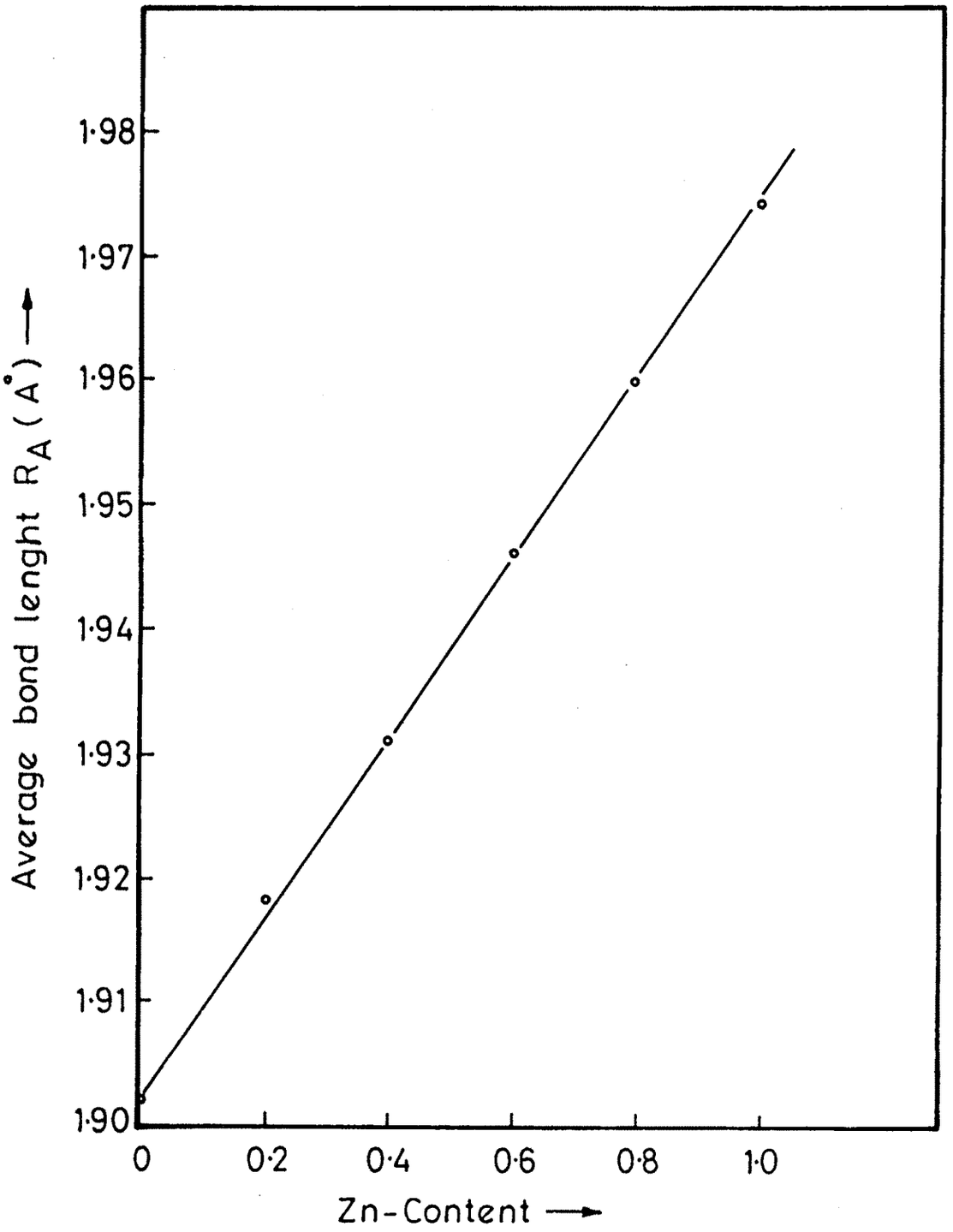

Fig. 2·10 Compositional variation of Average bond length R_A with Zn-content .

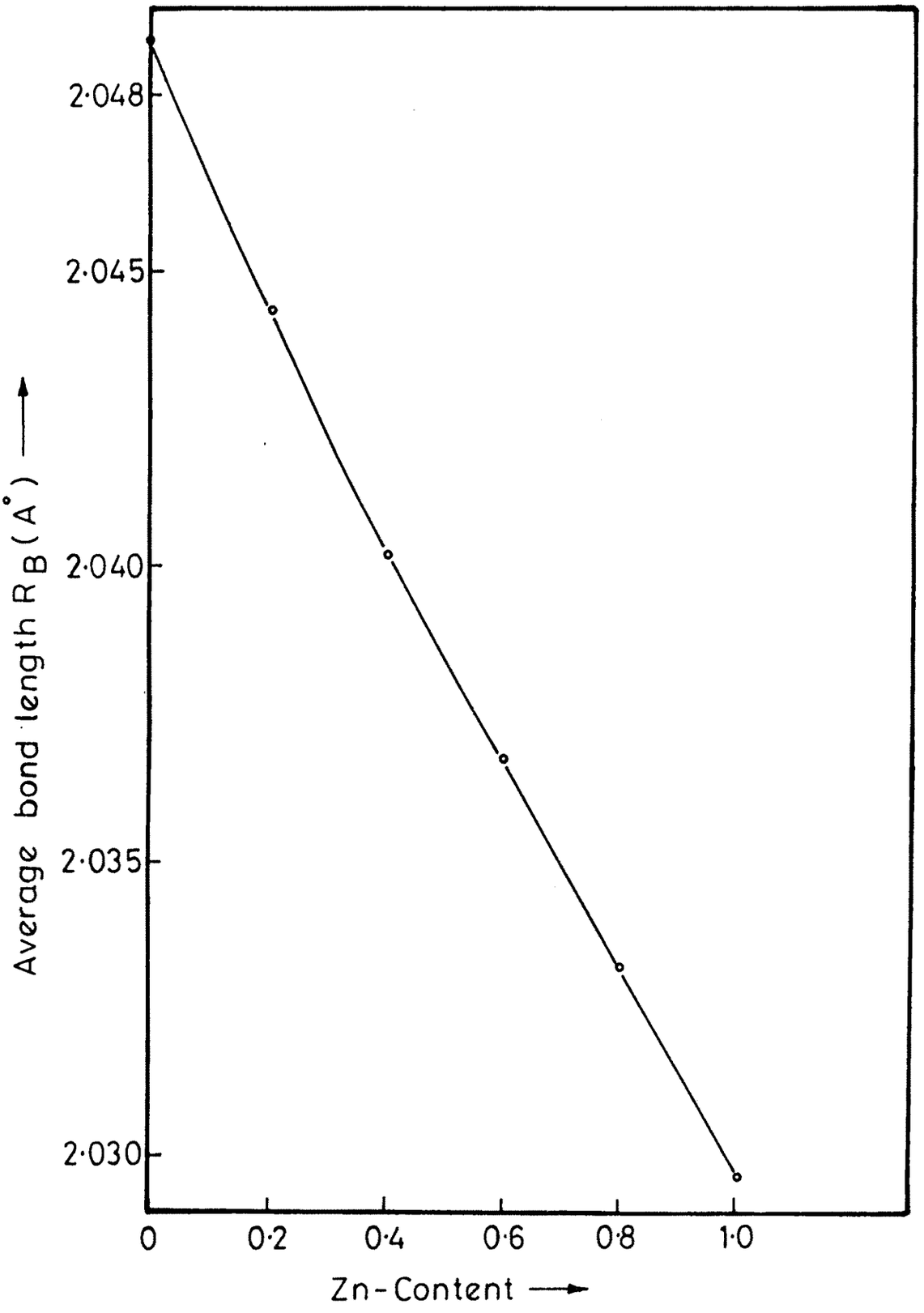

Fig.2·11 Compositional variation of Average bond length R_B with Zn-content.

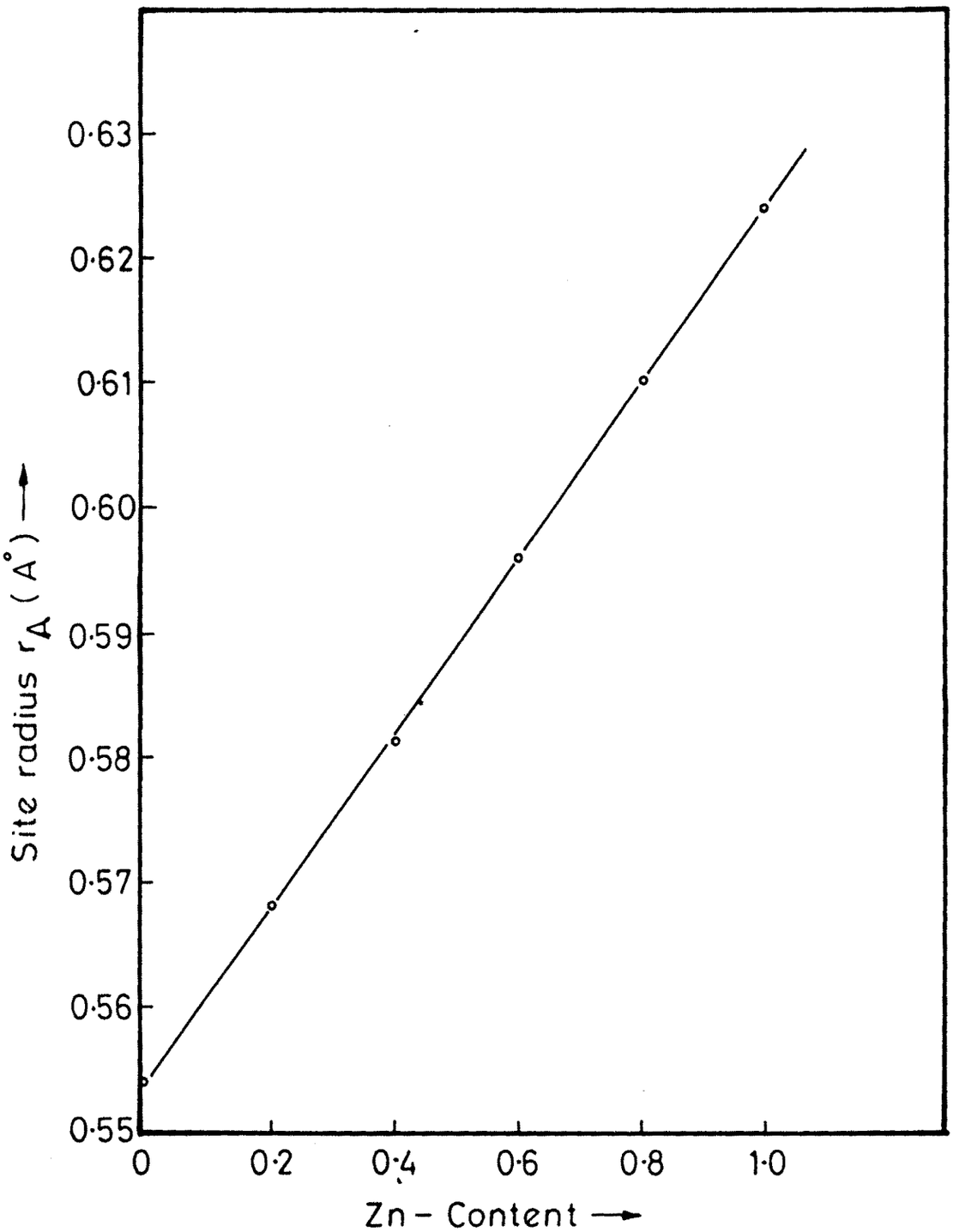

Fig.2·12 Compositional variation of site radius r_A with Zn-content .

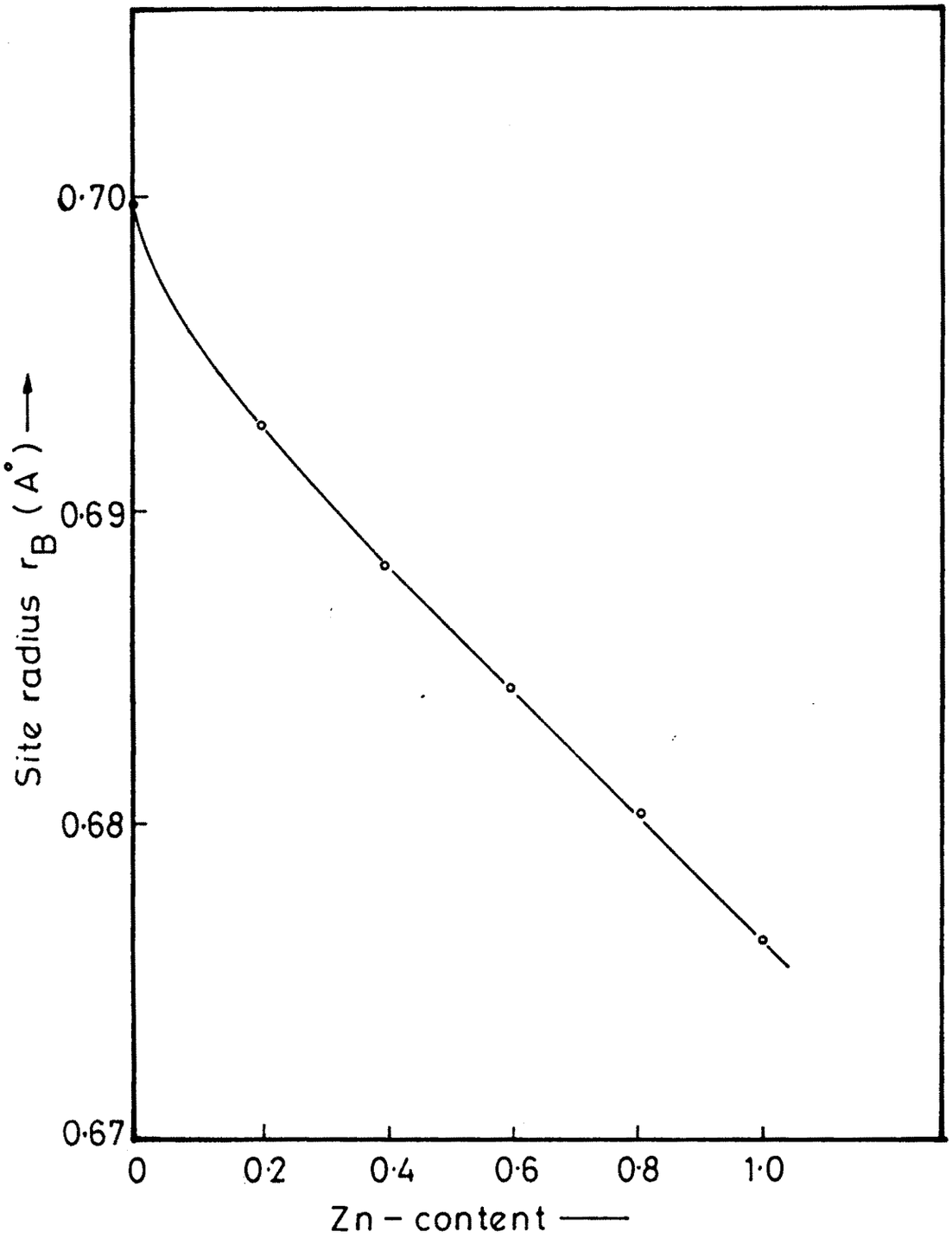

Fig. 2·13 Compositional variation of site radius r_B with Zn - content.

REFERENCES

[1] Takada Toshio and Kiyama, M.
Ferrites, Proc. Internat. Conf., Japan (1970),
P. 69 - 71.

[2] Kuczynski, C.G.
Ferrites, Proc. Internat. Conf., Japan (1970),
P. 87 - 95.

[3] Sato Toshihiko,
Ferrites, Proc. Internat. Conf., Japan (1970),
P. 72 - 74.

[4] Hilpert, S.
German Patents, 226, 347 (1909), 227, 787 (1909).

[5] Wagner, C.Z.
Phy. Chem. (b). 34, 309, (1936). "Diffusion and high temp. oxidation of metals, Atom movements". A.S.M. monographs. (Cleaveland).

[6] Schmalzried, H.Z.
Phy. Chem. (NF), 33, 111, (1962).

[7] Hauffe, K., Pschera, K.Z.
Anorg. Allgem. Chem. 262, 147 (1950).

[8] Snoek, J.L.
"New developments in ferromagnetic materials",
Elsevier Publ. Co., New York (1947).

[9] Gorter, E.W.
Proc. IRE. 42 (2), (1945).

[10] Boroth R.M.,
"Ferromagnetism", P.244-249,Van Nostrand Publ.Co.(1951).

[11] Vent J.J and Gorter E.W.,
Philips Tech. Rev., 13, 181 (1952).

[12] Wanger, C.Z.,
Phys. Chem., B-34, 309 - 16 (1936).

[13] Standley, K.J.
"Oxide magnetic materials", Clearendon Press, New York (1972), Chap. 2, P. 9.

[14] Economus, G.
J. Amer. Ceram. Soc. 38, 241, (1955).

[15] Swallow, D., Jordon, A.K.
Proc. Brit. Ceram. Soc., 2, 1 (1964).

[16] Murry. F., Lively, D.T. and William. J.
in "Ceramic Fabrication Processes", Ed. Kingery W.D.,
P. 147 - 71, Wiley (NY) (1958).

[17] Venkataramani, A.M., Aiyar R., Shekhar P.S.,
Bull Mater Sci. (India). Vol. 6, No-1, (1984).

[18] Coble, R.L., Burke, T.E.,
Progress in Ceramic Sci., Vol. III, P. 197, (1963).

[19} Oudemans, G.J.,
Philips Tech. Rev. 29, P. 45 (1968).

[20} Bragg W.L.,
Nature (London), 95, 561, (1915).

[21] Debye P. and Scherrer. F.
Physik, Z. 17, 277, (1916) and 18, 219 (1917).

[22] Cullity. B.D.
"Elements of X-ray diffraction". Addison Wesley Publ.
Co., INC. England (1959).

[23] Muthukumar Swamy. P., Nagarajan. T., and Narayan
swamy. A.,
J.Phys. C. (Solid State Phys). 5, (1982), 2519 - 2528.

[24] ASTM Cards. Wyckoff crystal structure data.

[25] Standley. K.J.,
"Oxide Magnetic Materials", Oxford Univ. Press, Amen.
House, London, E.C. 4, (1962), P. 24.

[26] Standley. K.J.,
"Oxide Magnetic Materials", Oxford Univ. Press, Amen.
House, London, E.C. 4, (1962) P. 21.

[27] Lavine B.F.,
Phys. Rev. (USA), B-7, 259, (1973).

[28] Dunitz J.D. and Orgel L.E.,
J.Phys. Chem. Solids 3 (GB), 318.